ARTICLES

Dynamical Host/Guest Interactions in Zeolites: Framework Isotope Effects on Proton Transfer Studied by Car−Parrinello Molecular Dynamics

Ettore Fois and Aldo Gamba*

Dip. di Chimica, Fisica, Matematica, Università degli Studi dell'Insubria, Sede di Como, Via Lucini 3, I-22100 Como, Italy

Received: March 19, 1998; In Final Form: January 13, 1999

Zeolites are microporous crystals of technological relevance, as they are used in many area as industrial catalysts, and the understanding of their behavior at the molecular level is of major interest. Differences in shape and compositions of the host crystals affect the reactivity of chemicals adsorbed in the pores of these materials, showing that host/guest interactions play a specific role. We report a Car−Parrinello study of sodium hydroxo sodalite dihydrate $Na_8[Al_6Si_6O_{24}](OH)_2 \cdot 2H_2O$ for the undoped crystal (^{28}Si) and the one doped with ^{30}Si. It is shown that differences in the relaxations of the framework atom oscillations, due to isotopic exchange, affect the relaxation of a proton transfer inside the zeolitic cage. The present results give an indication of "dynamical coupling" between one proton dynamics and its host crystalline matrix, which is effective only in the case of weak bonds.

1. Introduction

Zeolites are framework microporous crystals widely used as heterogeneous catalysts. They are characterized by an aluminosilicate lattice formed by SiO_4 and $AlO_4(TO_4)$ tetrahedra. The framework is built up by corner sharing TO_4 tetrahedra. The topology of the TO_4 framework allows the formation of molecular-sized cavities (cages and channels).[1,2] Chemicals in these cavities experience reaction fields different in different zeolites, due to various topologies and/or chemical composition (*host/guest* interactions at the molecular level).[3] This recalls the variation in reactivity of one compound in different solvents, where it is possible to observe different physicochemical behaviors as a response to changes in the environment. In the liquid phase, the study of solute/solvent interactions is entangled by the diffusive motion of both solute (reactant) and solvent. On the other hand, in zeolites the *solvent* is frozen and only solutes (adsorbed guests) can have diffusive behavior in the cages and channels of the crystals. Moreover, like in liquid solvents, zeolite's framework acts as a heat reservoir for the adsorbed molecules.[4,5] In liquids, it is customary to roughly divide the "solvent" effects into two main contributions, namely, a *static* contribution influencing the energetic of solutes; i.e., in a reaction R → P, the product P can be favored by stabilizing solute−solvent interactions with respect to reactant R. The latter contribution is the *dynamical* solvent effect due to the relaxation processes of the fluid's molecules which may influence reaction rates. This last effect could be of primary relevance in electron- and proton-transfer reactions,[6] where different solvent dielectric relaxations can alter the transfer rate and sometimes can even hinder the transfer process. These two effects may play a role in intracage processes in zeolites as well, and experimental evidence is now becoming available.[7] The static effect is easy to recognize, as a different cage size or a different Al/Si ratio alters the potential surface experienced by guest molecules. The dynamical contribution may be more subtle to be detected, and this general aspect extends to the focus of the present paper, the coupling of the motion of an $O_2H_3^-$ complex within a zeolite to the motion of the surrounding framework. First of all, zeolites are solid materials so that reorientational solvent-like processes are ruled out. However, the framework atoms oscillate around their crystallographic equilibrium positions, and the vibrations of the framework, which is in general electrically charged, may affect the motion of caged ionic and dipolar species. In a model calculation,[5] this host/guest dynamical coupling has been studied by tuning the potential of a guest molecule; it turned out that the relaxation of a sorbed diatomic is favored when the diatomic oscillates at frequencies close to the framework modes. This effect, when present, can be observed if one is able to change the way the framework atoms oscillate without changing the average framework structure, and this can be achieved by isotopic exchanges in the aluminosilicate zeolite structure. In a linear response regime,[8] this is equivalent to modifying the correlation functions of the framework atoms and examining if the correlation functions of guest species are affected by these changes. A different response function of guest species then indicates dynamical coupling between the host framework and its guest molecules. While in liquids the proper relaxation mechanisms can be described in terms of the orientational correlation functions of solvent molecules,[8] in solids and in zeolites in particular, velocity or dipole autocorrelation functions (or their Fourier Transform giving the power or IR spectra) are good candidates to describe this phenomenon.

We point out that the present study mainly is concerned with the motion of a proton shared between two OH^- and how its dynamics can be affected by the framework atoms motion,

10.1021/jp981569d CCC: $18.00
Published on Web 03/02/1999

without tackling the problem of the calculation of the proton-transfer reaction rate.[9]

As a result of their relevance, host/guest interactions in zeolites have been the subject of many studies in the past.[10] Moreover, with the introduction of the first-principles molecular dynamics method,[11] it is possible to enhance the accuracy of the study of both electronic and dynamical properties of complex systems. Recently, we have tried to explain intracage processes[12,13] by using the Car−Parrinello first-principles simulation techniques[11] to describe host/guest interactions in zeolites microscopically.

The Car−Parrinello approach has been recently used to study catalytic precursors in zeolitic cages, like the dynamics of the proton-transfer mechanism between an acid zeolite and a guest molecule like methanol.[14] We present here a Car−Parrinello[11] study of a zeolite (Sodalite) where a fast proton exchange occurs in a molecular complex, $O_2H_3^-$, not directly linked to the framework atoms. The dynamical "solvent" effect is studied by looking at the correlation functions of the guest complex when the aluminosilicate structure is doped with ^{30}Si and comparing the results with the correlation functions obtained for the undoped sodalite.

2. Method of Calculations

Sodium hydroxo sodalite dihydrate,[15] $Na_8[Al_6Si_6O_{24}](OH)_2 \cdot 2H_2O$, is the synthetic zeolite subject of our studies. It has the sodalite structure,[16] characterized by two cubooctahedral cages (β-cages) per crystallographic cell. The cages are connected by rings formed by four TO_4 units. There is a 1/1 ratio in Al/Si composition and perfect alternance in Al−O−Si bridges. The total charge of the aluminosilicate frame (six electrons per cell) is compensated by extraframework ions. Each β-cage contains four Na^+ ions arranged in a tetrahaedral cluster; in turn, each cationic cluster encapsulates a molecular complex, $O_2H_3^-$, so that the total charge in the cell is zero. Our simulation cell contains two β-cages. In our calculations of the protonated form, we have adopted the experimental lattice parameters and symmetry, namely, a cubic cell of 8.87 Å, with periodic boundary conditions. Electron−electron interaction is calculated by a gradient-corrected density functional approximation,[18] while norm conserving pseudopotentials[19] were used for the electron−ion interactions; H and Na atoms were treated with local pseudopotential, while d-nonlocality, in separable form,[20] was adopted for Al, Si, and O atoms. Wave functions were expanded in plane waves up to a cutoff of 60 Ry (electron density up to 240 Ry). A time step of 0.121 fs was used for the integration of the equations of motion. The simulations were performed with the silicon mass of 29.974 amu (^{30}Si) for the doped sodalite, while a mass of 28.086 amu (^{28}Si) was used, as in ref 12, for the undoped crystal. The masses of the other nuclei were fixed to their experimental values for both simulations. The same conditions and same technique[17] were used in the two simulations. Averages were gathered for both simulations for 4.8 ps, and the average temperatures for the two simulations were 140 and 139 K, respectively. We compare our results with experiments performed at 170 K;[15] however, as our simulations have been performed in the NVE microcanonical ensemble (at constant energy, volume, and particles number), the temperature is not fixed, the values of ∼140 K are the results of averages over the 4.8 ps elapsed time for each trajectory.

3. Results

3.1. Structural Analysis. Experimental data have been reported for the protonated and deuterated form of this zeolite.

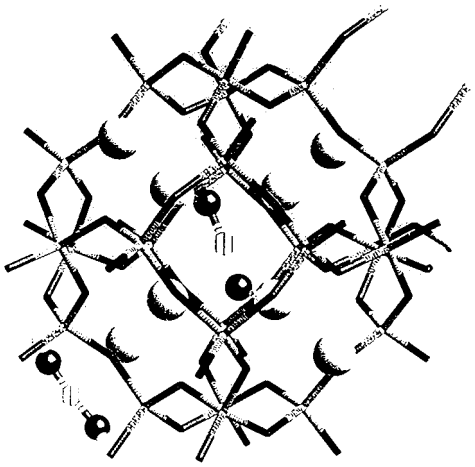

Figure 1. Snapshot of hydroxo sodalite dihydrate. One β-cage only is shown. The framework is represented by sticks; black sticks represent the framework oxygens, white sticks represent both the Al and Si atoms. Large white spheres represent Na cations, black spheres extraframework oxygens, and small white spheres represent protons. The H(1) protons are dashed white spheres.

Both experiments[15] (IR, NMR, X-ray and neutron diffractions) and a previous simulation[12] agree on the fact that the $O_2H_3^-$ complex, formally one H_2O and one OH^-, is actually formed by two OH^- and a shared third proton, jumping, on the femtoseconds scale, between the two OH^-. Following the definitions in ref 15, the protons forming the stable OH^- anions are labeled H(2), while the shared proton is labeled H(1). With T atoms, we refer to both Si and Al atoms of the framework.

No hydrogen bond has been found between the anions and the framework oxygens, meaning that each $O_2H_3^-$ anion is *floating* inside each sodium tetrahedron. From the electrostatic point of view, the crystal consists of a lattice of cages formed by shells of alternating positive and negative charges. A snapshot of the crystal is shown in Figure 1. Figures2 and 3 report some radial distribution functions ($g(r)$) calculated for the doped and undoped sodalite. They are compared with the $g(r)$ calculated from the experimental crystallographic positions.[15] It emerges that the calculated structures compare fairly well with the experimental geometry. Moreover, the ^{28}Si sodalite structure is practically identical to the one obtained for the ^{30}Si-doped crystal. This is not surprising if we take into account that the mass ratio of the two silicon isotopes is close to 1. In Figure 4, some of the distributions, $D(x)$, $D(y)$, and $D(z)$, of the crystallographic positions, calculated from the two simulations are reported. The $D(x_i)$'s are calculated folding the atomic positions back to fractional coordinates using the $P\bar{4}3n$ space group symmetry operations used for the X-ray and neutron diffractions refinements.[15] Figure 4 shows the experimental crystallographic coordinates as well. Here too, the calculated and experimental values compare well. However, differences emerge in the form of the distributions for the doped and undoped sodalites. While the $D(x_i)$'s for the undoped sodalite are unimodal, the distributions calculated for the ^{30}Si-doped structure are always bimodal. However, the first moments of the two sets of distributions $\langle x_i \rangle = \int x_i D(x_i)\, dx_i$ are practically identical, showing that the average atomic positions for the two simulations are the same, as can be inferred by the near identical structures of the $g(r)$'s. We believe that the origin of the bimodal distributions of the $D(x_i)$ for the heavier ^{30}Si sodalite is due to an incoming phase transition. The experimental X-ray and neutron diffractions studies are recorded at 170 K, and the same authors[15] say that below 150 K a series of (reversible) structural transitions occurr. It is possible that the doped structure is reaching one of the

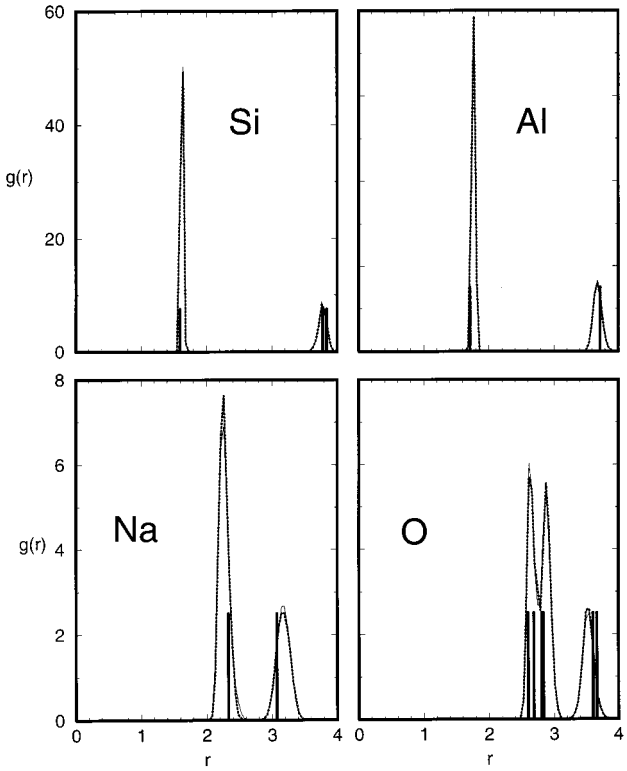

Figure 2. Calculated radial distribution functions $g(r)$ for the framework oxygens with Si, Al, Na, and with themselves. Continuous lines represent the $g(r)$'s for the ^{28}Si run; dotted lines represent the $g(r)$'s calculated for the ^{30}Si run. Vertical spikes show the corresponding experimental distances (in Å).

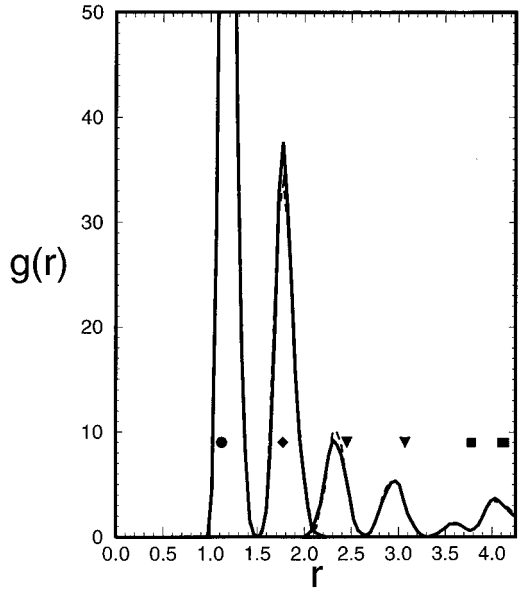

Figure 3. Calculated radial distribution functions $g(r)$ for H(1) atoms with the oxygen of the molecular complex $O_2H_3^-$, the H(2) hydrogens, the sodium atoms, and the framework oxygens. Continuous lines refer to the ^{28}Si run; dotted lines refer to the ^{30}Si run. Symbols correspond to the experimental distances: circle refers to oxygen, diamond to H, triangle to Na, and square to framework oxygens; distance in Å.

structural transitions as suggested by the bimodal (unstable) position distributions. As far as the guest complex is concerned, the present results confirm what was found both in a previous simulation[12] and in experiments,[15] namely, that there is a fast motion of the central (shared) proton and this motion is on the femtoseconds scale. In the $O_2H_3^-$ complex, the calculated oxygen−oxygen distance is 2.41 Å for both the doped and

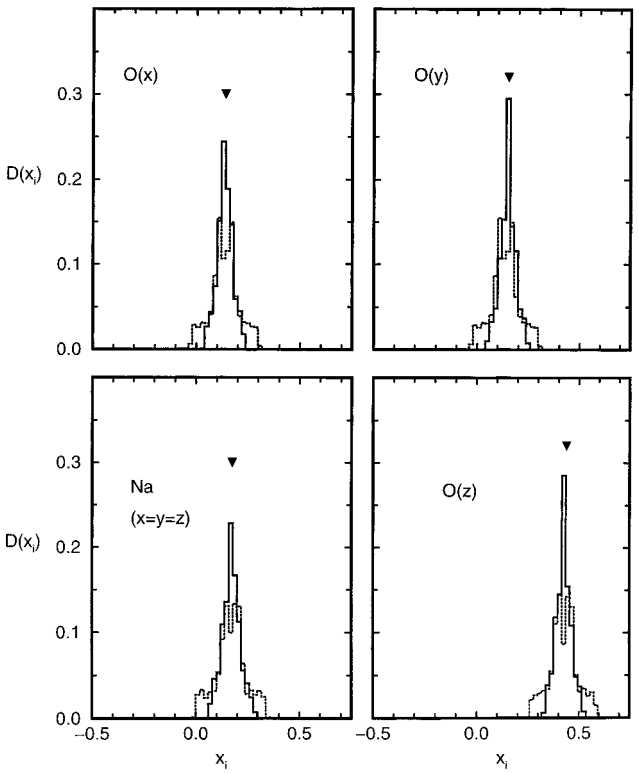

Figure 4. Calculated crystallographic coordinate distributions $D(x_i)$'s for the Na ($x = y = z$) and the x, y, and z $D(x_i)$'s for the framework oxygens. The experimetal values are quoted by triangles. Continuous lines refer to the ^{28}Si run; dotted lines refer to the ^{30}Si run.

undoped sodalites, to be compared with the X-ray data, 2.36 Å, and neutron data, 2.39 Å, for the protonated sample.

3.2. Dynamical Properties. It was found that the fast proton-transfer motion in the HO···H···OH complex encapsulated in the sodalite β-cage is correlated with the motion of the aluminosilicate framework.[12] This correlation was proposed as being due to couplings of the oscillations of the charged TO_4 lattice with the dynamics of the shared proton (H(1) in refs 12 and 15). These protons are located near the center of the β-cages, at a distance of ≥4 Å from T atoms (both Al and Si). We now compare correlation functions obtained from the simulation performed with the ^{28}Si isotope with the same functions obtained from the simulation with the ^{30}Si isotope. Figure 5 reports the velocity autocorrelation functions $C(t)$ of the H(1) protons in the two simulations. It emerges that the two correlations have different oscillation periods. This indicates that the H(1) response is different when the Si mass is changed. The differences are small, in line with the Si mass ratio (1.068). The isotopic substitution of atoms at such a distance is able to influence the motion of the H(1) protons, indicating a long-range coupling among the protons and the T atoms. Moreover, as the radial distribution functions $g(r)$ show that the average structures in the doped and undoped sodalites are the same, the different response of the H(1) protons should be related to the differences in the dynamics of the sodalite frame. In Figure 5, the H(1)'s $C(t)$ are compared with the Si's $C(t)$ calculated for the doped and undoped crystals. The dephasing of H(1) and Si $C(t)$'s in the two crystals are of comparable magnitude. A different behavior is observed for the protons forming the stable OH^- anions, H(2) protons in ref 15. The velocity autocorrelation functions for the silicon atoms and for the H(2) protons are shown in Figure 6. Here, the dephasing of the H(2)'s velocity autocorrelations in the two crystals is practically undetectable. This is due to the fact that the stronger OH bonds are less

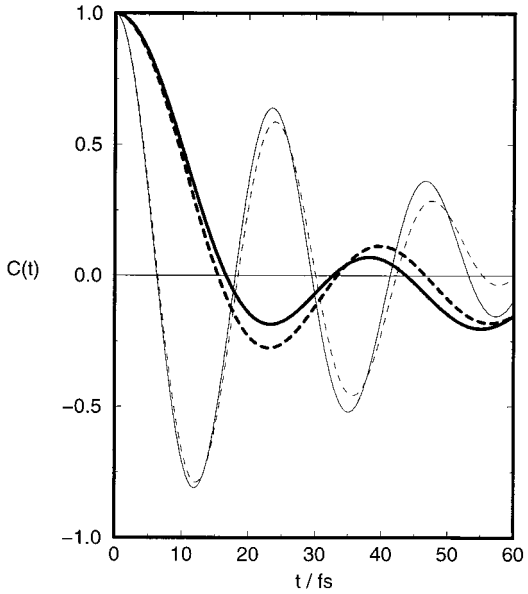

Figure 5. Velocities autocorrelation functions for T atoms (thick lines) and for H(1) atoms (thin lines). Continuous lines refer to the ^{28}Si simulation; dotted lines refer to the ^{30}Si one, respectively.

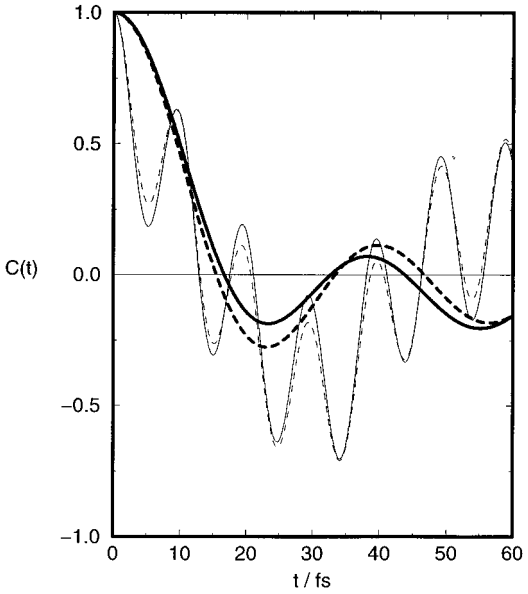

Figure 6. Velocities autocorrelation functions for T atoms (thick lines) and for H(2) atoms (thin lines). Continuous lines refer to the ^{28}Si simulation; dotted lines refer to the ^{30}Si one, respectively.

affected by the small pertubation induced by the $^{28}Si \rightarrow {}^{30}Si$ exchange than by the weaker O···H···O hydrogen bonds, which the shared proton is involved with. All these features can be appreciated in the frequency domain, by the Fourier transforms of the atomic velocities correlation functions, that give the power spectrum for the system, reported in Figure 7. The main features of the experimental (IR) spectrum are reproduced qualitatively by our calculated power (vibrational) spectra. A single band in the stretching region indicates the absence of water molecules. The experimental IR stretching frequency is 3650 cm^{-1}, while the calculated vibrational frequency is ∼3400 cm^{-1}. This large discrepancy, apart from approximations in the density functional theory, is mainly due to the fact that in the Car−Parrinello Lagrangean a fictitious inertia factor (500 au in our calculations) is assigned to the wave function coefficients,[11] this factor resulting in a fictitious enhancement of the real atomic mass with the consequence of reducing atomic oscillation frequencies.[21,22] This effect is more pronounced for light atoms, like hydrogen, and in the high-frequency zone of the spectrum. An atomic mass renormalization scheme has been proposed,[21] but as the physics is unaffected we adopted real masses for nuclei in our simulations.

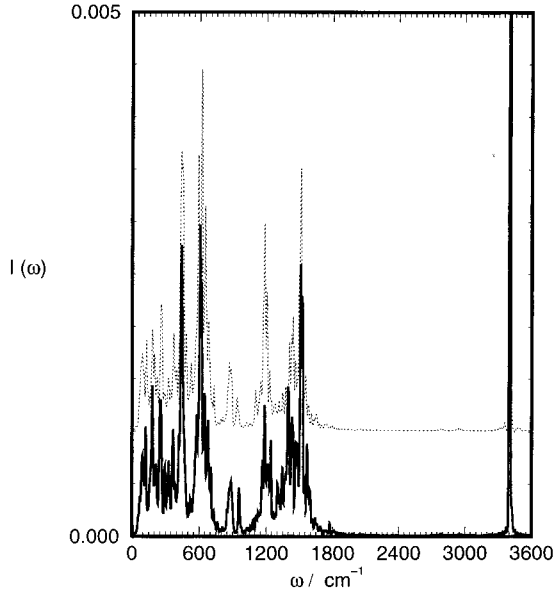

Figure 7. Fourier transform for the total velocity autocorrelation function (power spectrum). Continuous line refers to the ^{28}Si run; dotted line refers to the ^{30}Si run. The baseline of the latter is shifted upward. All spectra are normalized to 1.

The calculated power spectra present a set of bands in the 1000−1800 cm^{-1} region corresponding to the broad band peaked at ∼1500 cm^{-1} in the experimental spectrum, assigned to the H(1) vibrations, by both experiments[15] and simulations.[12] At lower frequencies, the framework bands give the major contribution to the spectra. If we now compare the spectra obtained from the two trajectories, we can confirm what is seen in the time domain. The high-frequency OH^- stretching mode is practically unaffected, the difference being 4 cm^{-1}, of the same order of the resolution of our calculated spectra (defined by the 4.8 ps elapsed time of the trajectories). However, some significant differences are present in the 1000−1800 cm^{-1} region and in the framework vibrational zone below 1000 cm^{-1}. These differences can be better understood by looking at partial spectra, i.e., spectra obtained by Fourier transforming velocity autocorrelation functions of groups of atoms. In Figure 8, the Fourier tranforms of the $C(t)$'s calculated from the T atom (Al and Si) velocities are shown and compared with the Fourier transforms of the $C(t)$'s for the H(1) protons for the two trajectories. These Fourier transforms are shown up to 1800 cm^{-1} because no bands are present at higher frequencies in these spectra. Below ∼950 cm^{-1}, some of the bands in the H(1) power spectra match those of the respective T atoms spectra, confirming what was previously found in a shorter (2.5 ps) simulation,[12] namely, that H(1) protons are "dancing" in tune with the framework atoms.

Some of the T atom bands are shifted due to the isotopic Si exchange. This is particular evident in Figure 9, where the same spectra are shown on different scales. It appears that the high-frequency bands of the T atoms (T−O stretching modes) are affected by isotopic substitutions, this effect being more pronounced in the highest wavenumber band where the contributions of the Si atoms is expected to be more relevant. The effect is lower in the lower frequency band, where the Al contribution is the relevant one. However, the shift observed in

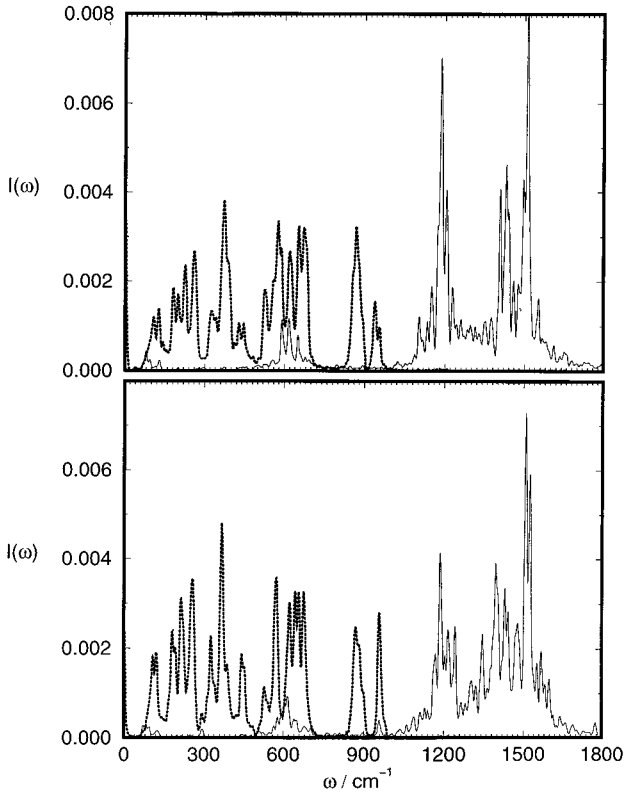

Figure 8. Top panel: Fourier transforms of the velocity autocorrelation functions for T atoms (dotted) and H(1) atoms (continuous) for the ^{30}Si run. Bottom panel: Fourier transforms of the velocity autocorrelation functions for T atoms (dotted) and H(1) atoms (continuous) for the ^{28}Si run. All transforms are normalized to 1.

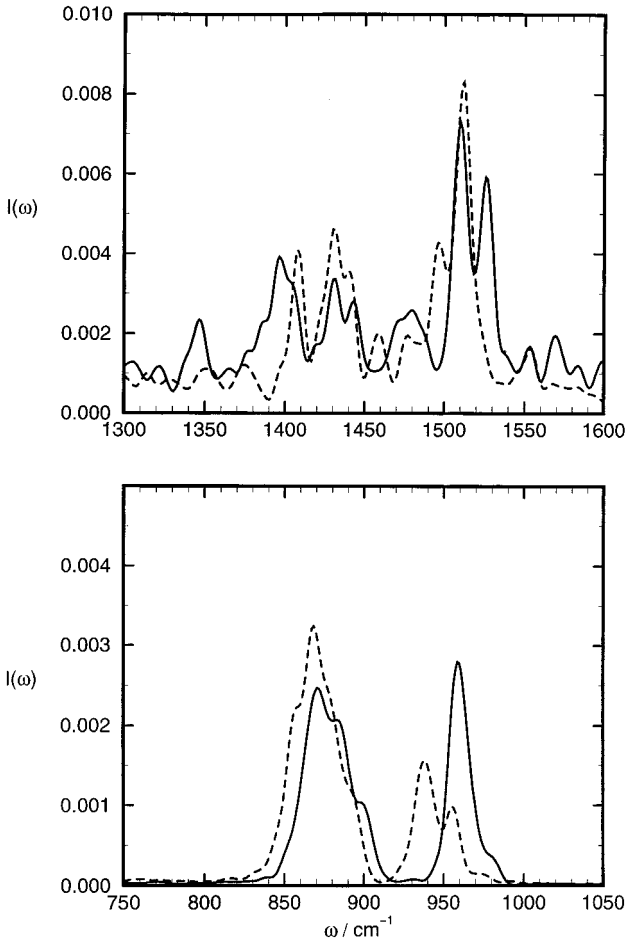

Figure 9. (top panel) Fourier transforms of the velocity autocorrelation functions for H(1) atoms. Continuous line refers to the ^{28}Si run; dotted line refers to the ^{30}Si run. (bottom panel) Fourier transforms of the velocity autocorrelation functions for T atoms. Continuous line refers to the ^{28}Si run; dotted line refers to the ^{30}Si run. All transforms are normalized to 1.

the 1000−1800 cm^{-1} region of the H(1) spectra calculated for the doped and undoped crystals can be only due to a long-range effect, as the isotope exchange occurs for atoms very far apart (≥4 Å). Also, the frequency shift of the H(1) protons (expecially in the case of the more intense doublet band centered at 1520 and 1502 cm^{-1} for the undoped and doped crystal, respectively) is of a magnitude comparable to that of the T atoms, and no T atom bands appear at these high frequencies.

Now some comments are due to the use of classical mechanics also for light particles such as protons. It has been shown that in the gas-phase quantum effects (e.g., tunneling) can influence the dynamics of a shared proton (like our H(1) protons). In the molecular complex $O_2H_3^-$ at 300 K, a free energy barrier is found for the proton exchange when classical mechanics is used, while the barrier disappears when quantum fluctuations are taken into account properly.[23] However, in $O_2H_5^+$, namely a proton shared between two H_2O molecules, the qualitative difference between classical and quantum treatment of the protons disappears.[23] It should be noticed that, in a quantum molecular dynamics study of $O_2H_5^+$,[24] it was found that, beyond a temperature dependence of the equilibrium geometry, the shared proton motion is coupled strongly to the other degrees of freedom in the complex. In this case, the shared proton oscillates between two water molecules and the frequency of its motion is distributed among a series of peaks in the range 1100−1800 cm^{-1}. In the hydroxo sodalite dihydrate, where the $O_2H_3^-$ anions are no longer in a vacuum but are in a solid charged matrix, the sodalite cages, nuclear quantum effects do not seem to play a qualitative role. This can be deduced by the experimental fact that the protonated and deuterated forms of the sodalite behave qualitatively in the same way.[15] Moreover, the experimental finding that the average oxygen−oxygen distance (in the HO···H···OH complex) decreases in the deuterated sample (2.39 and 2.29 Å for the protonated and deuterated sodalite, respectively) is generally interpreted as a single well potential structure for hydrogen bonds in condensed phases,[25] consequently ruling out the possibility of proton tunneling.

It has been argued[26] that current density functional approximations can underestimate proton-transfer energy barriers, but in this case, due to the very similar experimental behavior of the protonated and deuterated forms of hydroxosodalite,[15] such a barrier, if it exists at all, should be very low. Moreover, the good agreement between calculated and experimental results may give an a posteriori justification for using such an approximation. In this scenario, namely, very low or missing barrier for proton transfer and similar (experimentally found) proton/deuterium behavior, one may justify the use of classical mechanics for protons as well. Indeed, we believe that a proper quantum mechanical treatment for light particles[27,28] cannot change the main result of our calculations, i.e., the coupling of the shared proton motion with the zeolite framework dynamics.

4. Conclusions

The system studied here can be considered as a prototype for strong single symmetric minimum hydrogen bond,[25] and as proton transfer through hydrogen bond is a widespread phenomenon in a variety of areas, from material science to biology,

its understanding at the molecular level in a controlled environment, like in zeolites cages, could be of fundamental interest. The results of the simulations show that a proton-transfer process in a zeolite cage is intimately connected with the dynamics of the framework atoms. This behavior resembles the "dynamic solvent effects" in electron- and proton-transfer processes in the liquid phase, where orientational relaxations can modulate the transfer rates. In zeolites, however, solvent molecules diffusional and rotational motions are absent and the host/guest coupling is affected by the charged aluminosilicate framework dynamics. This coupling affects only weak bonds such as the hydrogen bonds in which the shared protons are involved. The effect, on the other side, is very weak or absent in the stronger bonds of the OH^- in the same cavities.

References and Notes

(1) Gottardi, G.; Galli, E. *Natural Zeolites*; Springer-Verlag: Berlin, 1985.

(2) Meier, W. M.; Olson, D. H. *Atlas of zeolite structure types*, 3rd ed.; Butterworth-Heinemann: London, 1992.

(3) Weitkamp, J. In *Proceedings of the 9th International Zeolite Conference*; von Ballmoos, R., Higgins, J. B., Treacy, M. M. J., Eds.; Butterworth-Heinemann: London, 1992; pp 13−46.

(4) Demontis, P.; Suffritti, G. B.; Fois, E.; Quartieri, S. *J. Phys. Chem.* **1992**, 96, 1482.

(5) Demontis, P.; Suffritti, G. B.; Tilocca, A. *J. Chem. Phys.* **1996**, *105*, 5586.

(6) Marcus, R. A. *Rev. Mod. Phys.* **1993**, *65*, 599; Heitle, H. *Angew. Chem., Int. Ed. Engl.* **1993**, *32*, 359. Scheiner, S. In *Proton Transfer in Hydrogen-Bonded Systems*; Bountis, T., Ed.; Plenum: New York, 1992. Staib, A.; Borgis, D.; Hynes, J. T. *J. Chem. Phys.* **1995**, *102*, 2487.

(7) Paze', C.; Bordiga, S.; Spoto, G.; Lamberti, C.; Zecchina, A. *J. Chem. Soc., Faraday Trans.* **1998**, *94*, 309.

(8) Madden, P. A. In *Liquids, Freezing and Glass Transition*; Hansen, J. P., Levesque, D., Zinn-Justin, J., Eds.; Elsevier Science Publishers: Amsterdam, 1991; pp 548−627.

(9) Cukier, R. E.; Zhu, J. *J. Phys. Chem. B* **1997**, *101*, 7180. Chandler, D. *Introduction to Modern Statistical Mechanics*; Oxford University Press: Oxford, 1987.

(10) Kahn, R.; Cohen de Lara, E.; Möller, K. D. *J. Chem. Phys.* **1985**, *83*, 2653; Suffritti, G. B.; Gamba, A. *Int. Rev. Phys. Chem.* **1987**, *6*, 299. Godber, J.; Ozin, G. A. *J. Phys. Chem.* **1988**, *92*, 2841. Zecchina, A.; Otero Areán, C. *Chem. Soc. Rev* **1996**, 187. Hong, S. B.; Camblor, M. A.; Davis, M. E. *J. Am. Chem. Soc.* **1997**, *119*, 761. Demontis, P.; Suffritti, G. B. *Chem. Rev.* **1997**, *97*, 2845.

(11) Car, R.; Parrinello, M. *Phys. Rev. Lett.* **1985**, *55*, 2471.

(12) Fois, E.; Gamba, A. *J. Phys. Chem.* B **1997**, *101*, 4487.

(13) Fois, E.; Gamba, A.; Maric, D. *Nuovo Cimento* D **1997**, *19*, 1679.

(14) Haase, F.; Sauer, J.; Hutter, J. *Chem. Phys. Lett* **1997**, *266*, 397.

(15) Wiebcke, M.; Engelhardt, G.; Felsche, J.; Kempa, P. B.; Sieger, P.; Schefer, J.; Fisher, P. *J. Phys. Chem.* **1992**, *96*, 392.

(16) Pauling, L. *Z. Kristallogr.* **1930**, *74*, 213. Hassan, I.; Grundy, H. D. *Acta Crystallogr.* **1983**, *C39*, 3.

(17) Hutter, J.; Ballone, P.; Bernasconi, M.; Focher, P.; Fois, E.; Goedecker, S.; Parrinello, M.; Tuckerman, M.; *CPMD Program*, version 3.0; MPI fur Festkörperforschung (Stuttgart) and IBM Research (Zürich), 1990−96.

(18) Parr, R. G.; Yang, W. *Density-Functional Theory of Atoms and Molecules*; Oxford University Press: Oxford, 1989. Becke, A. D. *J. Chem. Phys.* **1992**, *96*, 2155. Perdew, J. P. *Phys. Rev. B* **1986**, *33*, 8822.

(19) Troullier, N.; Martins, J. L. *Phys. Rev. B* **1991**, *43*, 1993.

(20) Kleinman, L.; Bylander, D. M. *Phys. Rev. Lett.* **1982**, *48*, 1425.

(21) Blöchl, P. E. *Phys. Rev. B* **1994**, *50*, 17953.

(22) Wathelet, V.; Champagne, B.; Mosley, D. H.; André, J.-M.; Massidda, S. *Chem. Phys. Lett.* **1997**, *275*, 506.

(23) Tuckerman, M. E.; Ungar, P. J.; von Rosenvinge, T.; Klein, M. L. *J. Phys. Chem.* **1996**, *100*, 12878. Tuckerman, M. E.; Marx, D.; Klein, M. L.; Parrinello, M. *Science* **1997**, *275*, 817.

(24) Cheng, H.-P.; Krause, J. L. *J. Chem. Phys.* **1997**, *107*, 8461.

(25) Novak, A. *Structure and Bonding 18*; Springer-Verlag: Berlin, 1974.

(26) Mijoule, C.; Latajka, Z.; Borgis, D. *Chem. Phys. Lett.* **1993**, *208*, 364.

(27) Pavese, M.; Chawla, S.; Lu, D.; Lobaugh, J.; Voth, G. A. *J. Chem. Phys.* **1997**, *107*, 7428.

(28) Tuckerman, M. E.; Laasonen, K.; Sprik, M.; Parrinello, M. *J. Chem. Phys.* **1995**, *103*, 150.